Arabian Journal for Science and Engineering (2022) 47:5073–5078
https://doi.org/10.1007/s13369-021-06394-w

RESEARCH ARTICLE-CIVIL ENGINEERING

The Effects of Calcium Aluminate Cement Substitution on Physicochemical Properties of Geopolymer–Zeolite Composites

Hee-Jeong Kim[1] · **Hammad R. Khalid**[2,3]

Received: 18 January 2021 / Accepted: 9 November 2021 / Published online: 10 January 2022

Abstract
Zeolites are porous aluminosilicate materials and are commonly used as adsorbents for various pollutants. Geopolymers made from industrial waste materials have an aluminosilicate structure similar to zeolites and can be converted to crystalline zeolites under high temperature and pressure conditions (hydrothermal conditions). The present study investigated the effects of fly ash substitution by calcium aluminate cement (CAC) in hydrothermally-treated geopolymer binders (often referred to as geopolymer-zeolite composites or geopolymer-supported zeolites). The substitution levels of fly ash by CAC were varied from 0 to 50% (0, 10%, 20%, 40%, or 50%). A mixture of waterglass and NaOH solutions was used for alkali activation of raw materials. The test results revealed that the CAC significantly affected the strength development and reaction products. All the CAC-substituted specimens showed significantly higher strength than fly ash-based control specimens. It was noted that the rise in compressive strength was mainly due to the formation of C–A–S–H gel in CAC-substituted specimens. The control specimens showed Na–P1 type zeolite while chabazite, faujasite, and hydroxysodalite phases were identified with incorporation of CAC. Hence, it was found that the CAC addition resulted in different Ca/Si molar ratios, which promoted the formation of different types of zeolites, thus these specimens can potentially be used for specific target applications.

Keywords Alkali-activated material (AAM) · Calcium aluminate cement (CAC) · Geopolymer–supported zeolite · Geopolymer–zeolite composite · Hydrothermal treatment · Fly ash

1 Introduction

Ordinary Portland cement (OPC) produces a large amount of carbon dioxide during its manufacturing process, while alkali-activated materials (AAMs) have advantages of recycling industrial by-products which mainly contain Ca, Al, and Si species [1, 2]. AAMs are known to possess comparable (sometime even better) strength and durability to OPC [1, 3]. Therefore, studies on the synthesis and applications of various types of AAMs are continuously increasing [4–7]. Geopolymers, classified as low-Ca AAMs, mainly consist of highly cross-linked zeolite-like amorphous aluminosilicate gel (N–A–S–H type) [3, 8]. This gel is the main strengthening constituent in geopolymers which has the tendency of converting to crystalline zeolites, specifically in high temperature conditions [9, 10]. Zeolites have a large porous structure and are frequently used as adsorbents for various pollutants. Conversion of geopolymeric gel into crystalline zeolites can open the possibility of their use for different applications (e.g., self-supported adsorbents or pervaporation membranes). Since geopolymeric gel acts as a supporting phase for zeolite crystals, they are often referred as geopolymer-supported zeolites or geopolymer–zeolite composites [8, 11, 12].

Since formation of zeolites can give a self-supporting system, this has attracted the attention of a number of researchers. Zeolite Na–P1, chabazite, faujasite, zeolite X, ZSM-20, and zeolite-like hydroxysodalite are some of the common crystalline phases that appear after hydrothermal treatment of gropolymeric binders [12]. Zeolite Na–P1 can effectively adsorb environmental pollutants such as SO_x,

✉ Hammad R. Khalid
hammad.khalid@kfupm.edu.sa; hrkhalid@kaist.ac.kr

1 Department of Civil and Environmental Engineering, Massachusetts Institute of Technology (MIT), Cambridge, MA 02139, USA

2 Civil and Environmental Engineering Department, King Fahd University of Petroleum and Minerals (KFUPM), Dhahran 31261, Saudi Arabia

3 Interdisciplinary Research Center of Building and Construction Materials, King Fahd University of Petroleum and Minerals (KFUPM), Dhahran 31261, Saudi Arabia

NO_x, Pb, and Hg [13–15]. Chabazite has high affinity to adsorb uranium radioactive ions and carbon monoxide [16, 17], while faujasite can effectively adsorb Pb, Co, and Cr, and also have ability to separate the hydrocarbon mixtures [18, 19]. Hydroxysodalite can absorb inorganic as well as organic pollutants with hydrophilic properties [20, 21]. This suggests that the formation of these phases in geopolymers can provide multifunctional materials. For instance, they can be potentially used as a construction material on sewage or for the removal of hazardous contaminants such as radionuclides or heavy metals. [22, 23].

Recently, Khalid et al. [8, 11] and Lee et al. [24] have reported works on typical two-step and robust one-step hydrothermal treatment methods for increasing the zeolites formation in geopolymeric binders. Their adsorption capacities were tested for lead and cesium removal, and promising results were obtained [8, 22]. It was highlighted that the elemental composition (mainly Si, Al, Na, and Ca content) and physical characteristics of raw materials play vital role in the reactions kinetics and resulting products. Specifically, Ca/Si and Al/Si molar ratios were found to affect the strength development as well as formation of different crystalline phases [11, 24]. Similar findings were also reported by Simao et al. [25]. Moreover, the Ca/Si ratio is also reported to affect the degree of silicate polymerization, which contributes to the production of main cement hydrates such as C–S–H and C–A–S–H [26]. Specimens with higher Si content generally showed increase in strength, while variation of Ca content resulted in formation of different zeolitic phases in addition to its effects on strength. Hence, this study focused on systematically investigating the effects of varying elemental composition on the reaction products. Calcium aluminate cement (CAC), which has higher CaO and Al_2O_3 content, was added at increasing percentages to vary the starting Ca/Si, Al/Si, and Si/Na molar ratios. Their effects on developing crystalline phases and mechanical strength were analyzed and discussed.

2 Materials and Methods

The calcium aluminate cement (CAC) and class F fly ash (FA), used in this study, were procured from Union cements and Hadong coal-fired power plant, South Korea, respectively. The chemical compositions of raw materials were measured by XRF and are given in Table 1. A mixture of waterglass and 6 M NaOH solution was used as activator. The waterglass had 1.38 g/mL specific gravity, 29 wt.% SiO_2, 10 wt.% Na_2O, and 61 wt.% H_2O. The NaOH/waterglass and activator/binder weight ratios of 0.5 and 1.0 were used for all the specimens, respectively. In the starting mixture, up to 50% of FA (0, 10%, 20%, 40%, or 50%) was replaced by CAC. Table 2 shows the specimens mix proportions and their starting compositions in terms Ca/Si, Si/Al, and Si/Na molar ratios. The one-step method, proposed by Khalid et al. [8], was used for synthesis of self-supported zeolites as follows: (1) the mixture was homogeneously mixed for 15 min at ambient temperature, (2) the mixed slurry was poured into 25 × 25 × 25 mm Teflon molds, and (3) the Teflon molds were placed into autoclave for the hydrothermal treatment for 48 h. The hydrothermal treatment system consists of 60 °C temperature for 6 h and 150 °C temperature for next 42 h. Specimens were demolded after hydrothermal treatment and were put at 25 °C for further curing up to 7 and 28 days.

Table 1 Chemical composition of raw fly ash and calcium aluminate cement

(Qt.%)	SiO_2	Al_2O_3	CaO	Fe_2O_3	MgO	Na_2O	SO_3	TiO_2	P_2O_5	K_2O
Fly ash	57.0	21.0	4.8	10.0	1.3	–	1.0	1.5	1.5	1.4
CAC	4.83	50.77	38.39	1.82	0.40	0.63	0.24	2.04	–	–

Table 2 Mix proportion of the specimens

Sample name	Control (F)	C10	C20	C40	C50
Fly ash	100	90	80	60	50
CAC	0	10	20	40	50
Ca/Si	0.077	0.142	0.219	0.427	0.570
Al/Si	0.371	0.460	0.565	0.847	1.042
Si/Na	2.612	2.396	2.182	1.761	1.553

To investigate the physicochemical characteristics of synthesized specimens with CAC substitutions, compressive strength and X-ray diffractometry (XRD) tests were conducted. The compressive strength was measured in accordance with ASTM C109, using a 50 kN universal testing machine. The XRD analysis was conducted by using a high-resolution X-ray diffractometer manufactured by PANalytical with CuK at 40 kV and 30 mA within a scan range of 5°–60° 2θ. Phase identification was done using the International Center for Diffraction Data (ICDD) PDF database.

3 Results and Discussion

3.1 Crystalline Phases

The XRD results of 7-day and 28-day cured specimens are shown in Fig. 1. The zeolite Na–P1, PDF#01-074-1787 was observed in all the specimens. This is the most common zeolitic phase synthesized by activation of fly ash, mainly due to the favored Si/Al molar ratio of fly ash as observed in many studies [27–29]. The control sample showed the highest quartz, PDF #01-086-1629 and mullite, PDF #01-

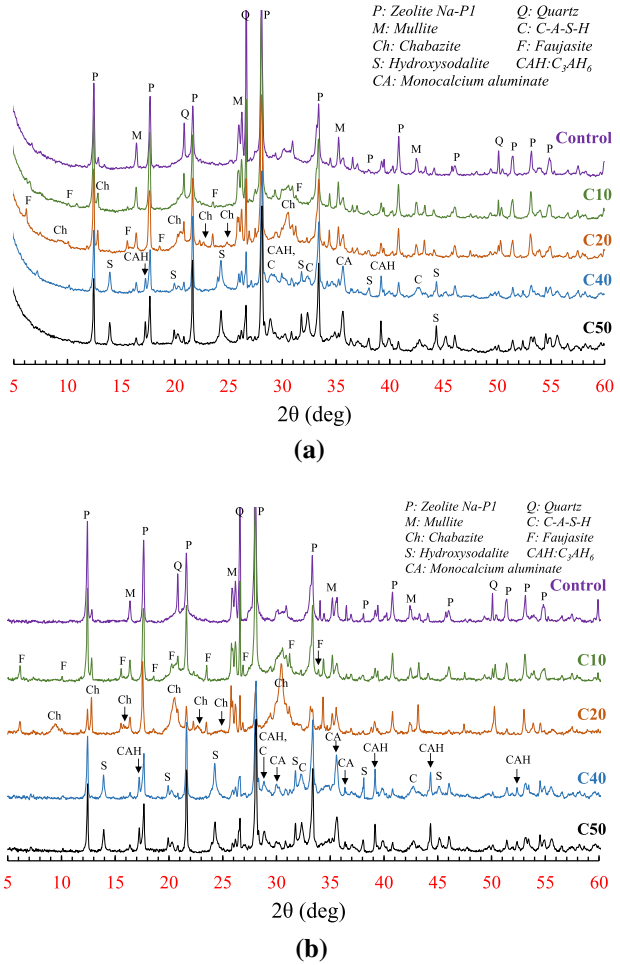

Fig. 1 XRD patterns of calcium aluminate cement incorporated geopolymer-supported zeolites **a** 7-day and **b** 28-day cured specimens

074-4145 peaks than other specimens. Quartz and mullite are the inherited phases of raw fly ash, and their reactivity during alkali activation is reported to be low, hence mostly present in alkali-activated fly ash-based binders [30]. After the substitution of fly ash with CAC, a decrease in relevant peaks was evident as the fly ash content was decreasing.

With substitution of CAC, sample C10 showed small peaks of faujasite (PDF # 00-038-0232, 01-074-2761) and chabazite (PDF #00-002-0062, 00-019-1178, 01-086-1567) phases, in addition to zeolite Na–P1 which could be mainly attributed to the increase in Ca/Si molar ratio [31, 32]. The C20 specimens showed the highest intensity of chabazite peaks which further verified the effect of increased Ca/Si molar ratio. The C–A–S–H gel (PDF #04-017-1483, 00-033-0306) peaks became more evident in C40 and C50 specimens. Furthermore, instead of zeolitic phases, the zeolite-like hydroxysodalite (PDF #00-039-0219, 01-071-5356) and calcium aluminate hydrate C_3AH_6 (PDF # 01-072-1109) were observed in C40 and C50 specimens. The higher calcium content has been reported to hinder the formation of zeolites. Sugano et al. [33] synthesized zeolites using low-Ca slags, while Ca-rich slag resulted in formation of tobermorite and hydrogarnet. Wajima et al. [34] reported that the high Ca content ash cannot be converted to zeolites, instead it results in formation of hydroxysodalite. Similar results were observed by the authors in the previous studies [8, 11, 24]. Moreover, C_3AH_6 is a high density hydrogarnet which form through conversion of metastable hydrates of Ca-rich CAC (CAH_{10} and C_2AH_8), especially in high temperature and humidity conditions [35]. The direct appearance of C_3AH_6 hydrate peaks can be attributed to the hydrothermal conditions used in this study.

Zeolite Na–P1, faujasite, chabazite, and hydroxysodalite all have three-dimensional network with different crystalline structures. Zeolite Na–P1 has gismondine (GIS) structure with single four- and eight-membered rings, while hydroxysodalite (sodalite hydrate) has SOD structure with single four- and six-membered rings [31]. Faujasite (FAU) contains SOD-cages which are linked with the double six-membered rings (D6R), and chabazite has CHA structure containing D6R members [12, 36]. Moreover, chabazite and hydroxysodalite belong to ABC-6 family, whose formation has been reported in concentrated NaOH solutions [1, 10, 36].

Several studies have reported that faujasite and chabazite have shown high adsorption capacities for cations [12, 37, 38]. On the other hand, hydroxysodalite is geometrically more flexible because of the lack of hydrogen bonding in the structure so that ion exchange can occur more actively compared to sodalite [39]. In addition, high Al/Si molar ratio in hydroxysodalite might lead to high cation exchange capacity due to the presence of more negative charges in the structure [40, 41]. Hence, the formation of different crystalline phases in the synthesized specimens can potentially open the possibility of their use for capture of different species. In light of the literature, potential uses of synthesized specimens are categorized in Table 3.

3.2 Mechanical Strength

The 7- and 28-day compressive strength values of synthesized specimens, along with the effects of Ca/Si and Al/Si molar ratios, are shown in Fig. 2. The 7-day compressive strength of control, C10, C20, C40, C50 specimens were 3.64, 4.38, 15.22, 16.03, and 10.03 MPa, respectively. All the CAC-substituted specimens showed higher strength than the control specimen. Recently, Lach et al. [42] studied the effects of CAC addition on fly ash-based geopolymers. Similar behavior was observed by the authors i.e., compressive strength increased with CAC content [42]. Another study by Temuujin et al. [43] reported the effects of adding different calcium compounds (i.e., calcium oxide and calcium hydroxide) on the mechanical strength of fly ash-based

Table 3 Types of zeolite and possible applications of the specimens

Types of zeolite	Applications	Control	C10	C20	C40	C50
Zeolite Na–P1	Adsorption of environmental pollutants (SO_x, NO_x, Pb, Hg, etc.) [13–15]	✓	✓	✓	✓	✓
Faujasite	Adsorption of Heavy metal ion (Pb, Co, and Cr) [16, 17]		✓	✓		
Chabazite	Adsorption of radioactive ions, carbon monoxide [16, 17]		✓	✓		
Hydroxysodalite	Adsorption of inorganic and organic pollutants [20, 21]				✓	✓

*Zeolites found in each sample were marked (✓) in table

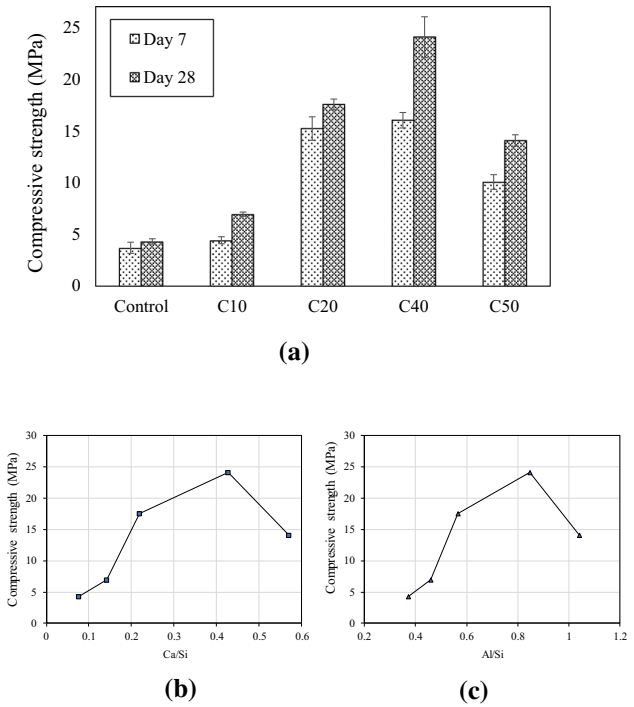

Fig. 2 Compressive strength of the specimens **a** and its correlation with Ca/Si **b** and Al/Si **c** molar ratios

geopolymers. It was found that the addition of calcium oxide and calcium hydroxide, both resulted in increased compressive strength [43].

As discussed in the previous section, Ca plays vital role in the formation of different reaction products and development of microstructure. It is known that the precursor with higher Ca content (such as slag) promotes the formation of C–A–S–H type gel, resulting in higher mechanical strength [44–46]. As the incorporation of CAC increased, the Ca/Si molar ratios increased (from 0.077 to 0.570) and so does the compressive strength. This was possibly the main reason of higher strength of CAC-substituted specimens, despite the fact that Al/Si molar ratio was also increasing. Normally, higher silica content (low Al/Si molar ratio) is desired for high strength geopolymers, but this is the case when N–A–S–H-type gel is the main strengthening phase [11]. Since CAC-substitution formed more C–A–S–H–type gel, hence higher strength was achieved in these specimens. The C40 specimens with 40% CAC substitution showed the highest compressive strength. However, strength decreased with further addition of CAC in C50 specimens. The Si content became too low in C50 (Si/Al < 1) which possibly resulted in weaker C–A–S–H matrix, or the strength contribution from N–A–S–H gel possibly decreased as well due to formation of weaker Si–O–Al bonds [47]. The measured compressive strength values of the specimens might seem lower compared to a typical cementitious binder used for structural applications; however, these values are more than enough for their potential utilization as self-supported bulk-type adsorbents for adsorption of different contaminants as tabulated in Table 3.

4 Conclusions

The effects of CAC substitution on physicochemical properties of geopolymer-supported zeolite composites were investigated in this study. The results of this study suggest that an increase in CAC content results in enhanced compressive strength owing to the formation of C–A–S–H gel. Sample C40 with 40% CAC content showed the highest compressive strength, while further increased to 50% CAC resulted in strength decrease. The crystalline phases also evolved with increase in Ca/Si and Al/Si molar ratios. In addition to zeolite Na–P1, faujasite and chabazite appeared in C10 and C20 specimens, which changed to hydroxysodalite and calcium aluminate hydrate C_3AH_6 in C40 and C50 specimens. Since all these crystalline phases have distinct structures and potential for different applications as summarized, the specimens synthesized in this study can be used for a number of applications. This study provided an insight that how starting composition can be varied to synthesize different crystalline products. Further studies should follow the detailed characterization and demonstration of potential applications.

Acknowledgements The authors would like to acknowledge the support provided by the Deanship of Scientific Research (DSR) at King Fahd University of Petroleum and Minerals (KFUPM) under Grant SR191025.

Funding Funding was provided by King Fahd University of Petroleum and Minerals (Grant No. SR191025).

References

1. Duxson, P.; Fernández-Jiménez, A.; Provis, J.L.; Lukey, G.C.; Palomo, A.; Van Deventer, J.S.J.: Geopolymer technology: The current state of the art. J. Mater. Sci. **42**, 2917–2933 (2007). https://doi.org/10.1007/s10853-006-0637-z
2. Gartner, E.: Industrially interesting approaches to "low-CO2" cements. Cem. Concr. Res. **34**, 1489–1498 (2004). https://doi.org/10.1016/j.cemconres.2004.01.021
3. Provis, J.L., van Deventer, J.S.J. (eds.) Alkali Activated Materials: State-of-the-art Report, RILEM TC 224-AAM, vol. 13. Springer, Dordrecht (2014). https://doi.org/10.1007/978-94-007-7672-2.
4. Yeddula, B.S.R.; Karthiyaini, S.: Experimental investigations and prediction of thermal behaviour of ferrosialate-based geopolymer mortars. Arab. J. Sci. Eng. **45**, 3937–3958 (2020). https://doi.org/10.1007/s13369-019-04314-7
5. Kumar, M.L.; Revathi, V.: Microstructural properties of alkali-activated metakaolin and bottom ash geopolymer. Arab. J. Sci. Eng. **45**, 4235–4246 (2020). https://doi.org/10.1007/s13369-020-04417-6
6. Alghannam, M.; Albidah, A.; Abbas, H.; Al-Salloum, Y.: Influence of critical parameters of mix proportions on properties of MK-based geopolymer concrete. Arab. J. Sci. Eng. **46**, 4399–408 (2021). https://doi.org/10.1007/s13369-020-04970-0
7. Wang, H., Zhu, Z., Pu, S., Song, W.: Solidification/stabilization of Pb^{2+} and Cd^{2+} contaminated soil using fly ash and GGBS based geopolymer. Arab. J. Sci. Eng. (2021). https://doi.org/10.1007/s13369-021-06109-1
8. Khalid, H.R.; Lee, N.K.; Park, S.M.; Abbas, N.; Lee, H.K.: Synthesis of geopolymer-supported zeolites via robust one-step method and their adsorption potential. J. Hazard. Mater. **353**, 522–533 (2018). https://doi.org/10.1016/j.jhazmat.2018.04.049
9. Park, S.M.; Khalid, H.R.; Seo, J.H.; Yoon, H.N.; Son, H.M.; Kim, S.H., et al.: Pressure-induced geopolymerization in alkali-activated fly ash. Sustainability **10**(3538), 11 (2018). https://doi.org/10.3390/su10103538
10. Oh, J.E.; Jun, Y.; Jeong, Y.: Characterization of geopolymers from compositionally and physically different Class F fly ashes. Cem. Concr. Compos. **50**, 16–26 (2014). https://doi.org/10.1016/j.cemconcomp.2013.10.019
11. Khalid, H.R., Lee, N.K., Choudhry, I., Wang, Z., Lee, H.K.: Evolution of zeolite crystals in geopolymer-supported zeolites: effects of composition of starting materials. Mater. Lett. (2019). https://doi.org/10.1016/j.matlet.2018.12.044.
12. Rożek, P.; Król, M.; Mozgawa, W.: Geopolymer–zeolite composites: a review. J. Clean. Prod. **230**, 557–579 (2019). https://doi.org/10.1016/j.jclepro.2019.05.152
13. Querol, X.; Moreno, N.; Umaa, J.C.; Alastuey, A.; Hernández, E.; López-Soler, A., et al.: Synthesis of zeolites from coal fly ash: an overview. Int. J. Coal Geol. **50**, 413–423 (2002). https://doi.org/10.1016/S0166-5162(02)00124-6
14. Woolard, C.D., Petrus, K., Van der Horst, M.: The use of a modified fly ash as an adsorbent for lead. Water SA (2000)
15. Wdowin, M.; Wiatros-Motyka, M.M.; Panek, R.; Stevens, L.A.; Franus, W.; Snape, C.E.: Experimental study of mercury removal from exhaust gases. Fuel (2014). https://doi.org/10.1016/j.fuel.2014.03.041
16. Warchoł, J.; Matłok, M.; Misaelides, P.; Noli, F.; Zamboulis, D.; Godelitsas, A.: Interaction of U aqVI with CHA-type zeolitic materials. Microp. Mesop. Mater. (2012). https://doi.org/10.1016/j.micromeso.2011.12.045
17. Mortier, W.J.; Pluth, J.J.; Smith, J.V.: Positions of cations and molecules in zeolites with the chabazite framework II Adsorption of carbon monoxide on dehydrated Ca-exchanged chabazite. Mater. Res. Bull. (1977). https://doi.org/10.1016/0025-5408(77)90095-2
18. Nikolakis, V.; Xomeritakis, G.; Abibi, A.; Dickson, M.; Tsapatsis, M.; Vlachos, D.G.: Growth of a faujasite-type zeolite membrane and its application in the separation of saturated/unsaturated hydrocarbon mixtures. J. Membr. Sci. (2001). https://doi.org/10.1016/S0376-7388(00)00623-2
19. Maiti, M.; Sarkar, M.; Xu, S.; Das, S.; Adak, D.; Maiti, S.: Application of silica nanoparticles to develop faujasite nanocomposite for heavy metal and carcinogenic dye degradation. Environ. Prog. Sustain. Energy (2019). https://doi.org/10.1002/ep.12904
20. Esaifan, M.; Hourani, M.; Khoury, H.; Rahier, H.; Wastiels, J.: Synthesis of hydroxysodalite zeolite by alkali-activation of basalt powder rich in calc-plagioclase. Adv. Powder Technol. (2017). https://doi.org/10.1016/j.apt.2016.11.002
21. Kazemimoghadam, M.; Mohammadi, T.: Mechanisms and experimental results of aqueous mixtures pervaporation using nanopore HS zeolite membranes. Desalination (2010). https://doi.org/10.1016/j.desal.2010.06.004
22. Lee, N.K.; Khalid, H.R.; Lee, H.K.: Adsorption characteristics of cesium onto mesoporous geopolymers containing nano-crystalline zeolites. Microp. Mesop. Mater. **242**, 238–244 (2017). https://doi.org/10.1016/j.micromeso.2017.01.030
23. Van Der Bruggen, B.; Vandecasteele, C.; Van Gestel, T.; Doyen, W.; Leysen, R.: A review of pressure-driven membrane processes in wastewater treatment and drinking water production. Environ. Prog. **22**, 46–56 (2003). https://doi.org/10.1002/ep.670220116
24. Lee, N.K.; Khalid, H.R.; Lee, H.K.: Synthesis of mesoporous geopolymers containing zeolite phases by a hydrothermal treatment. Microp. Mesop. Mater. **229**, 22–30 (2016). https://doi.org/10.1016/j.micromeso.2016.04.016
25. Simão, L.; De Rossi, A.; Hotza, D.; Ribeiro, M.J.; Novais, R.M.; Klegues Montedo, O.R., et al.: Zeolites-containing geopolymers obtained from biomass fly ash: influence of temperature, composition, and porosity. J. Am. Ceram. Soc. **104**, 803–815 (2021). https://doi.org/10.1111/jace.17512
26. Jamsheer, A.F.; Kupwade-Patil, K.; Büyüköztürk, O.; Bumajdad, A.: Analysis of engineered cement paste using silica nanoparticles and metakaolin using 29Si NMR, water adsorption and synchrotron X-ray diffraction. Constr. Build. Mater. (2018). https://doi.org/10.1016/j.conbuildmat.2018.05.272
27. Inada, M.; Eguchi, Y.; Enomoto, N.; Hojo, J.: Synthesis of zeolite from coal fly ashes with different silica–alumina composition. Fuel (2005). https://doi.org/10.1016/j.fuel.2004.08.012
28. Bakharev, T.: Geopolymeric materials prepared using Class F fly ash and elevated temperature curing. Cem. Concr. Res. **35**, 1224–1232 (2005). https://doi.org/10.1016/j.cemconres.2004.06.031
29. Steenbruggen, G.; Hollman, G.G.: The synthesis of zeolites from fly ash and the properties of the zeolite products. J. Geochem. Explor. (1998). https://doi.org/10.1016/S0375-6742(97)00066-6
30. Park, S.M.; Jang, J.G.; Lee, N.K.; Lee, H.K.: Physicochemical properties of binder gel in alkali-activated fly ash/slag exposed to high temperatures. Cem. Concr. Res. **89**, 72–79 (2016). https://doi.org/10.1016/j.cemconres.2016.08.004
31. IZA. International Zeolite Association 1973. http://www.iza-online.org/. Accessed 3 Nov 2020

32. Minerals.net. https://www.minerals.net/mineral/chabazite.aspx. Accessed 3 Nov 2020
33. Sugano, Y.; Sahara, R.; Murakami, T.; Narushima, T.; Iguchi, Y.; Ouchi, C.: Hydrothermal synthesis of zeolite A using blast furnace slag. ISIJ Int. **45**, 937–945 (2005). https://doi.org/10.2355/isijinternational.45.937
34. Wajima, T.; Shimizu, T.; Ikegami, Y.: Zeolite synthesis from paper sludge ash with addition of diatomite. J. Chem. Technol. Biotechnol. **83**, 921–927 (2008). https://doi.org/10.1002/jctb.1893
35. Son, H.M.; Park, S.; Kim, H.Y.; Seo, J.H.; Lee, H.K.: Effect of $CaSO_4$ on hydration and phase conversion of calcium aluminate cement. Constr. Build. Mater. **224**, 40–47 (2019). https://doi.org/10.1016/j.conbuildmat.2019.07.004
36. Baerlocher, C., McCusker, L.B.: Database of zeolite structures. Available at http://www.iza-structure.org/databases/ (2014)
37. Liu, Y.; Yan, C.; Zhang, Z.; Wang, H.; Zhou, S.; Zhou, W.: A comparative study on fly ash, geopolymer and faujasite block for Pb removal from aqueous solution. Fuel **185**, 181–189 (2016). https://doi.org/10.1016/j.fuel.2016.07.116
38. Grey, T.J.; Nicholson, D.; Gale, J.D.; Peterson, B.K.: A simulation study of the adsorption of nitrogen in Ca-chabazite. Appl. Surf. Sci. **196**, 105–114 (2002). https://doi.org/10.1016/S0169-4332(02)00042-9
39. Oh, J.E.; Moon, J.; Mancio, M.; Clark, S.M.; Monteiro, P.J.M.: Bulk modulus of basic sodalite, $Na8[AlSiO_4]$ $6(OH)_2{\cdot}2H_2O$, a possible zeolitic precursor in coal-fly-ash-based geopolymers. Cem Concr Res (2011). https://doi.org/10.1016/j.cemconres.2010.09.012
40. Munthali, M.W.; Elsheikh, M.A.; Johan, E.; Matsue, N.: Proton adsorption selectivity of zeolites in aqueous media: effect of Si/Al ratio of zeolites. Molecules (2014). https://doi.org/10.3390/molecules191220468
41. Baek, W.; Ha, S.; Hong, S.; Kim, S.; Kim, Y.: Cation exchange of cesium and cation selectivity of natural zeolites: chabazite, stilbite, and heulandite. Microp. Mesop. Mater. (2018). https://doi.org/10.1016/j.micromeso.2018.01.025
42. Lach, M.; Korniejenko, K.; Walter, J.; Stefanska, A.; Mikula, J.: Decreasing of leaching and improvement of geopolymer properties by addition of aluminum. Materials (Basel) **13**(495), 1–9 (2020)
43. Temuujin, J.; Van, R.A.; Williams, R.: Influence of calcium compounds on the mechanical properties of fly ash geopolymer pastes. J. Hazard. Mater. **167**, 82–88 (2009). https://doi.org/10.1016/j.jhazmat.2008.12.121
44. Kim, G.M.; Khalid, H.R.; Kim, H.J.; Lee, H.K.: Alkali activated slag pastes with surface-modified blast furnace slag. Cem. Concr. Compos. (2017). https://doi.org/10.1016/j.cemconcomp.2016.11.009
45. Kim, G.M., Khalid, H.R., Park, S.M., Lee, H.K.: Flow property of alkali-activated slag with modified precursor. ACI Mater. J. **114**, 867–876 (2017). https://doi.org/10.14359/51700794
46. Li, Z.; Liu, S.: Influence of slag as additive on compressive strength of fly ash-based geopolymer. J. Mater. Civ. Eng. **19**, 470–474 (2007). https://doi.org/10.1061/(ASCE)0899-1561(2007)19:6(470)
47. Kim, E.H.: Understanding effect of silicon/aluminum ratio and calcium hydroxide on chemical composition, nanostructure and compressive strength for metakaolin geopolymers. University of Illinois at Urbana-Champaign (2012)